Journal of Mining and Metallurgy, 46 A (1) (2010) 1 - 10

Journal of
Mining and
Metallurgy

GEOCHEMICAL ANOMALY SEPARATION BY CONCENTRATION-AREA FRACTAL MODEL IN BARDASKAN AREA, NE IRAN

Mehdi Hashemi[*], Peyman Afzal[#], Iraj Rasa[***], Mousa Noghreian[****], Khosro Khosro Tehrani[*] and Mansour Vosoughi Abedini[*]**

[*]Department of Geology, Science and Research branch, Islamic Azad University (IAU), Tehran, Iran
[**]Department of Mining Engineering, South Tehran branch, Islamic Azad University, (IAU), Tehran, Iran
[***]Shahid Beheshti University, Earth Sciences Faculty, Tehran, Iran
[****]Department of Geology, Isfahan University, Isfahan, Iran

(Received 14 September 2010; accepted 13 December 2010)

Abstract

Geochemical anomaly separation using the concentration-area (C-A) method at Bardaskan area, NE Iran, is studied in this paper. Lithogeochemical data sets were used in this geochemical survey which was conducted for the exploration for Au and Cu mineralization in Bardaskan area. There are two main mineralization concluded epithermal gold mineralization and a disseminated system. Anomalous thresholds values for the mineralized zone were computed based on the data obtained from chemical analysis of samples for the lithological units. Several anomalies at local scale were identified for Au (13 ppb), Cu (40 ppm), Ag (2.3 ppm), As (4 ppm) and Fe (6920 ppm) the obtained results suggests existence of local Au and Cu anomalies whose magnitude generally is above 630 ppb and 5000 ppm, respectively. The most important mineralization events are responsible for presence of Au and Cu at grades above 631 ppb and 5012 ppm. The study shows threshold values for Au and Cu are being a consequence of the occurrence of anomalous accumulations of silicification and phyllic alterations metamorphic rocks especially in tuffaceous sandstones and sericite schist types. The obtained results were compared with fault distribution patterns reveals a positive direct correlation between mineralization in anomalous areas and the faults present in the mineralized system.

Key words: *geochemical anomaly, epithermal system, concentration-area method, multifractal, Bardeskan, NE Iran.*

[#] ***Corresponding author:*** *peymanafzal@yahoo.com*

1. Introduction

Separation of anomalies from background is a fundamental issue in geochemical exploration operation. In the last century, customized statistical methods usually assumed that the concentration of chemical elements in the crust follow a normal or log-normal distribution. A geochemical anomaly as defined is a region where the concentration of a specific element is greater than a certain threshold value by statistical parameters, such as mean, median, mode, and standard deviation [5, 7, 15]. But, statistical methods e.g., by histogram analysis or Q-Q plots assuming normality or lognormality and do not consider the shape, extent and magnitude of anomalous areas and disregard its spatial variability [19]. Furthermore, the gathered data have to be modified in traditional methods such as rejection of outliers and normalization of data.

Fractal models can be established by Benoit Mandelbrot (1983), which he has applied to objects that were too irregular to be described by ordinary Euclidean geometry [9, 10, 17]. Fractal theory has been applied to mineral resources studies since late 1980s [1, 3, 6, 12, 14, 18, 20, 21, 22]. Recently, Cheng et al. (1994) proposed concentration-area (C-A) method based on the elemental geochemical distributions and occupy areas relationships. This idea and premise provided a scientific tool to demonstrate that an empirical relationship between concentration-area (C-A) does exists [3, 6, 8, 11, 13, 20]. Cheng et al. (1994) showed that there are various parameters which have a key role in spatial distributions of most of the elements for a given geological-geochemical environments.

In this paper, Bardaskan area Cu, Au, Ag, As and Fe anomalies are separated by concentration-area method. Subsequently, a general discussion is argued whereby the anomalous threshold values are correlated to the relevant structural, lithological, and alteration data and this may explain how obtained results were derived.

2. The concentration-area method

The concentration-area (C-A) method serves to illustrate the relationship correlated between the obtained results with the geological, geochemical and mineralogical information. Its most useful features are the easy implementation and the ability to compute quantitative anomalous thresholds [6, 13].

Cheng et al. (1994) proposed the concentration–area (C–A) method for separating geochemical anomalies from background in order to characterize the distribution of elemental concentrations. This model has the general form [6]:

$$A(\rho \leq \upsilon) \infty \rho^{-a1} ; A(\rho \geq \upsilon) \infty \rho^{-a2} \quad (1)$$

Where $A(\rho)$ denotes the area with concentration values greater than the contour value ρ; υ represents the threshold; and a_1 and a_2 are characteristic exponents. Using fractal theory, Cheng et al. (1994) derived similar power-law relationships and equations in extended form [6]. The area $A(\rho)$ for a given ρ is equal to the number of cells multiplied by cell area with concentration values greater than ρ. Average concentration values are used for those boxes containing more than one sample. Area-concentration [A (ρ)] with element concentrations greater than ρ usually shows a power-law relation [6]. The breaks between straight-line segments on this plot and the corresponding values of ρ have been used as cut-offs to separate geochemical values into different components, representing different causal factors, such as geological differences, geochemical processes and mineralizing events [16].

3. Geological setting of the Bardaskan area

The Bardaskan area of about 7.5 km^2 is situated about 16 km N of Bardaskan in NE Iran, as depicted in Fig. 1. This area is located in Taknar zone, which is one of the subdivisions of Iranian central structural zone at north Darouneh fault [2]. Bardaskan mineralized area includes Au epithermal system and Cu disseminated system [4].

__Figure 1.__ Location of studied area in NE Iran (Black square)

The study area is mainly comprised of Ordovician volcanic, metamorphic and volcano-clastics rocks from Taknar zone. Volcanic rocks are included rhyolite, rhyodacite, diabase and spillite. Also, the metamorphic rocks, including metasand-stone, schist especially sericite schist and chlorite schist, and slates are existed in the area. Tuffaceous sandstones and schists are extended in this area.

The main structural features are two faults system trending NE-SW and E-W. Locally, their feather type fractures and joints are intense, as presented in Fig. 2. The main alteration zones of phyllic, silicification, chloritization and sericitiza-tion types were accompanied by the quartz-sulfides vein to veinlets fillings of quartz.

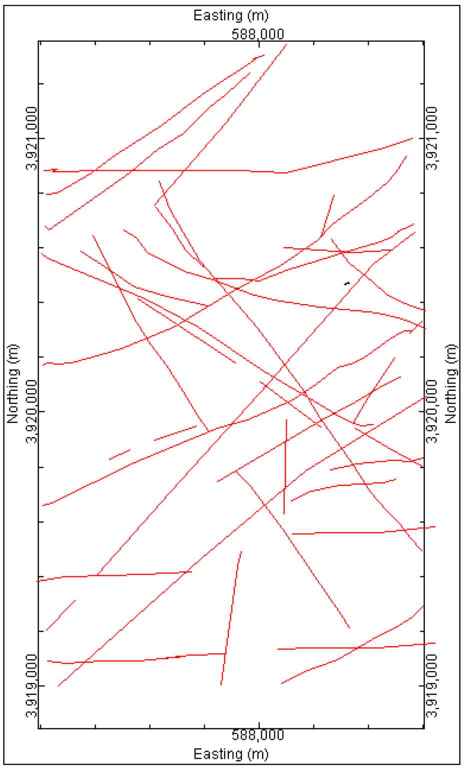

__Figure 2.__ Faults distribution map of Bardaskan study area

The ore minerals, i.e. chalcopyrite and pyrite and native Au are present and, the latter ones occurred in the zone of quartz veins and sericite alteration (Fig. 3). Precise extension and relationships between alteration zones and mineralization, and economical evaluation of the area are still being investigated and is under study.

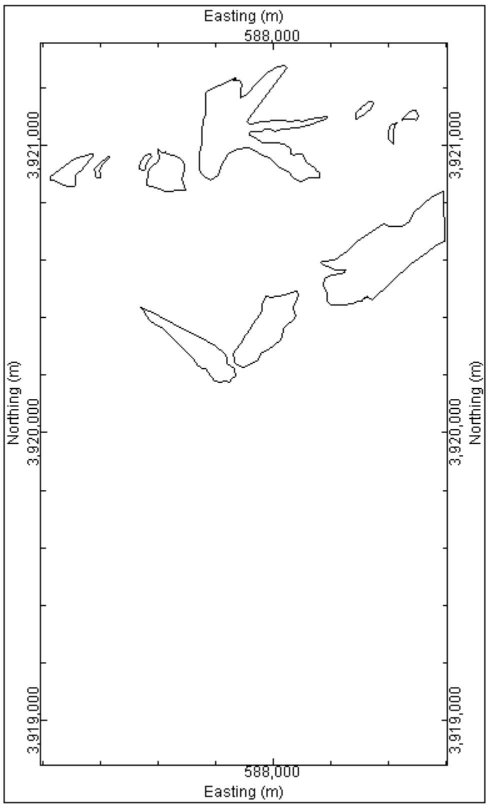

Figure 3. *Alteration and accompanied mineralization map of Bardaskan study area*

4. Litho geochemistry

Total of 483 collected lithogeochemical samples were analyzed by ICP-MS for elements which relate to Au and Cu mineralization and are of interest, and Ag, As and Fe concentrations were of no significance. Fig. 4 is the location map of the samples. Statistical results show that Au, Cu, As, Ag and Fe mean values are 38.2 ppb, 436.5, 10.3, 1.2 ppm and 3.9%, respectively. Their distributions are as shown in Fig. 5 and are not normal and variation between maximum and minimum for these data show a wide range.

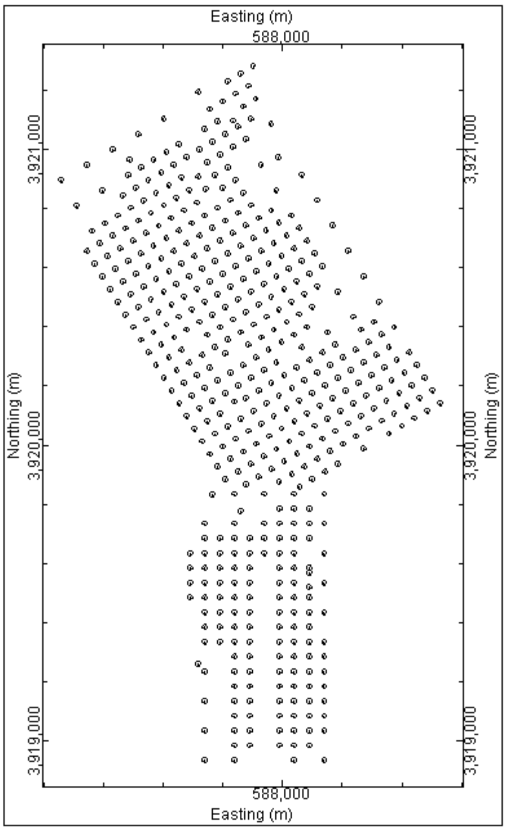

Figure 4. *Lithogeochemical samples location map of Bardaskan area*

Geochemical maps were generated with IDS (Inverse Distance Squared) method by RockWorks™ v. 14 software package. The area was gridded by 20 m×20 m cells. Carrying on this procedure is not cumbersome because there is a regular gridding of 20 m×20 m cells.

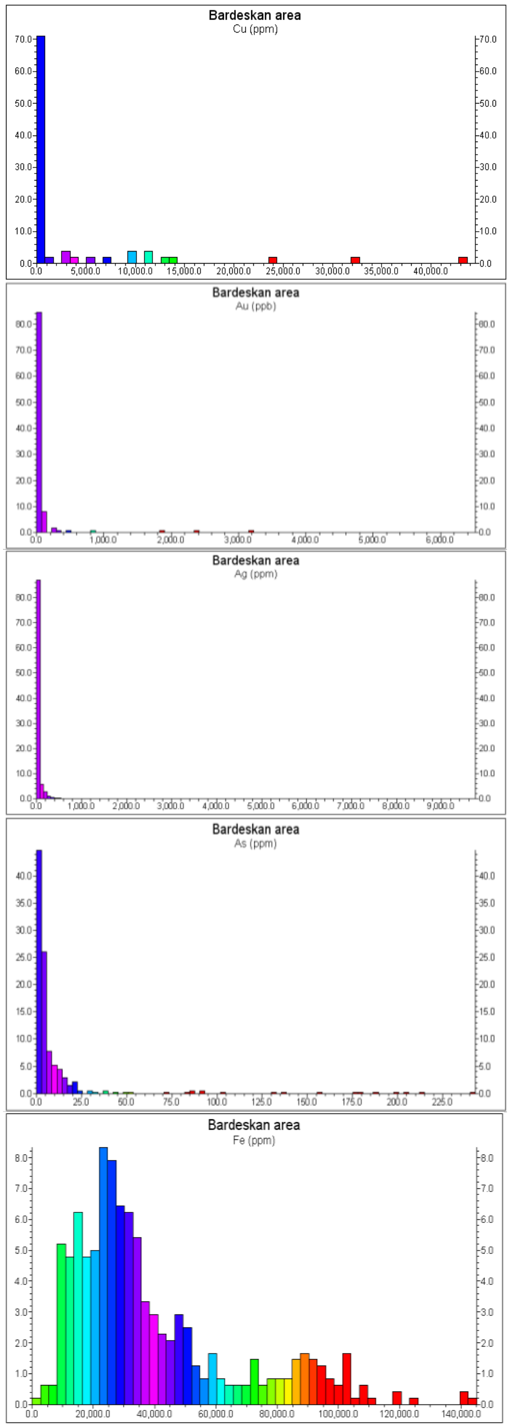

Figure 5. *Cu, Au, Ag, As and Fe histograms*

The evaluated grades in cells were sorted out based on decreasing grades and cumulative areas were calculated for grades. Finally, log-log plots were constructed for Au, Cu, Ag, As and Fe (Fig. 6).

Geochemical populations are delineated in these plots of Au, Cu, Ag, As and Fe. On the basis of this procedure, there are 4 populations for Au and Ag and 3 populations for Cu, As and Fe, respectively as shown in Fig. 6. Cu anomalous threshold is 40 ppm and its high intensity anomaly is 5012 ppm. Also, it is clear that there are three stages of Cu enrichments based on log-log plot (Fig. 6).

The first event for Cu C-A variations occurred at grades below 40 ppm. The second event shows up between grades 40 ppm and 5012 ppm. The final event included major Cu mineralization which occurred and interpreted in grades higher than 5012 ppm. Au threshold and high intensity anomalies are 13 ppb, and 631 ppb, as shown in Fig. 6. Au log-log plot shows that major Au enrichment occurred at 631 ppb and higher. Ag anomalous threshold is about 1.1 ppm. There are two enrichment steps interpreted as seen in C-A log-log plot of Au and Ag in Fig. 6. Major Ag enrichment started from 2.3 ppm, and, 13.2 ppm concentration is beginning of high intensity Ag anomaly.

Each geochemical population in this study was assumed to have various kinds of distributions, and its various components, such as individual chemical elements and their concentrations could be fitted into a straight line on log-log plot.

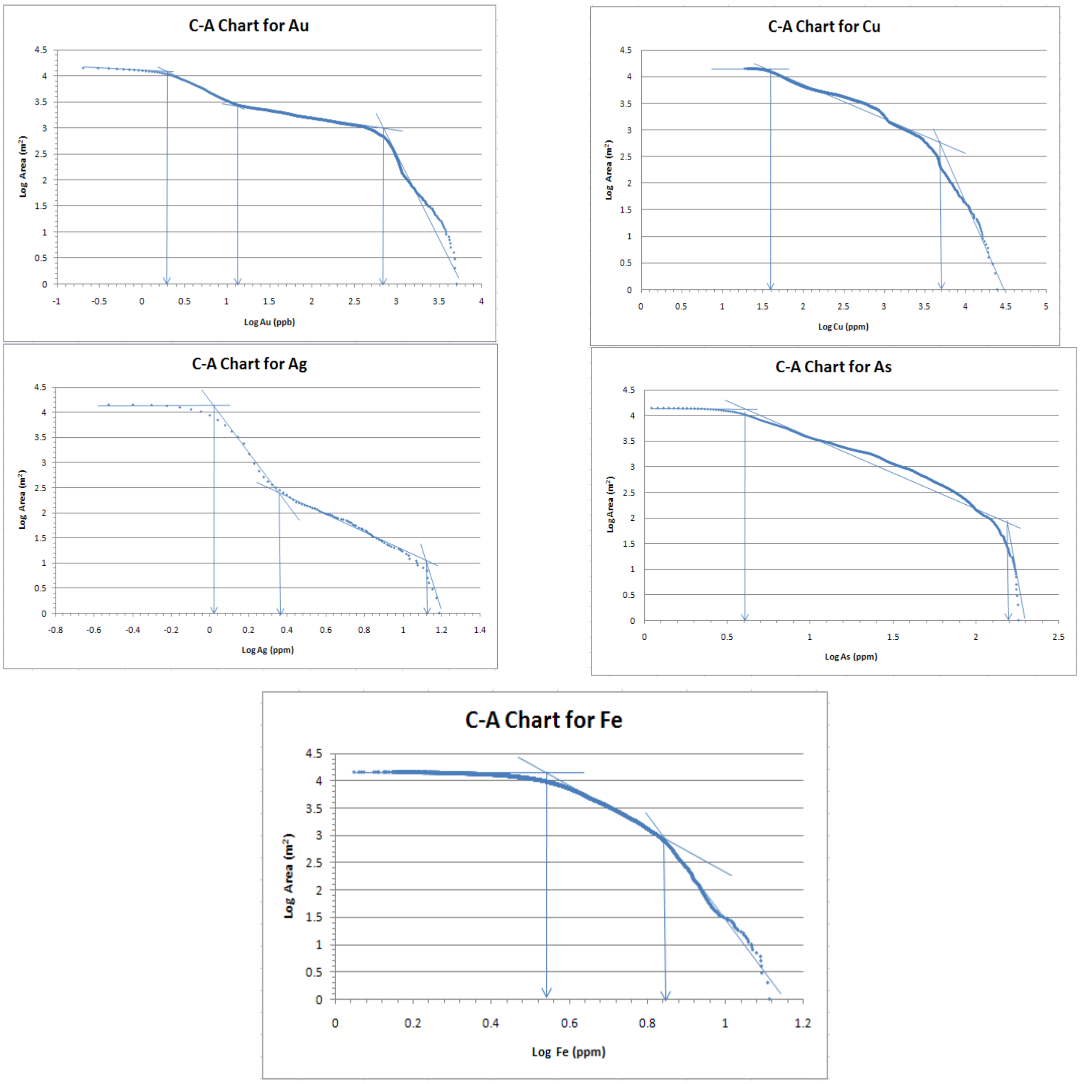

Figure 6. *Log-log plots (C-A method) for Au, Cu, Ag, As and Fe. The vertical axis represents cumulative cell areas A(ρ), with elemental concentration values greater than ρ, and the horizontal axis is the actual values (ρ)*

Obviously due to non-uniform behavior of the elements, if plotted on log-log coordinates, the plot will have different slopes and various straight line segments which connects them at them an angle or with breaks on the plot. Breaks between the straight-line segments and the corresponding values of Au, Cu, Ag, As and Fe have been used as cutoffs to reclassify cell values in the IDS interpolated maps are presented in Fig. 7. Clearly locations of Au anomalies are in northern, eastern and central parts of the area and the high intensive anomalies are situated in NE parts as depicted in Fig. 7.

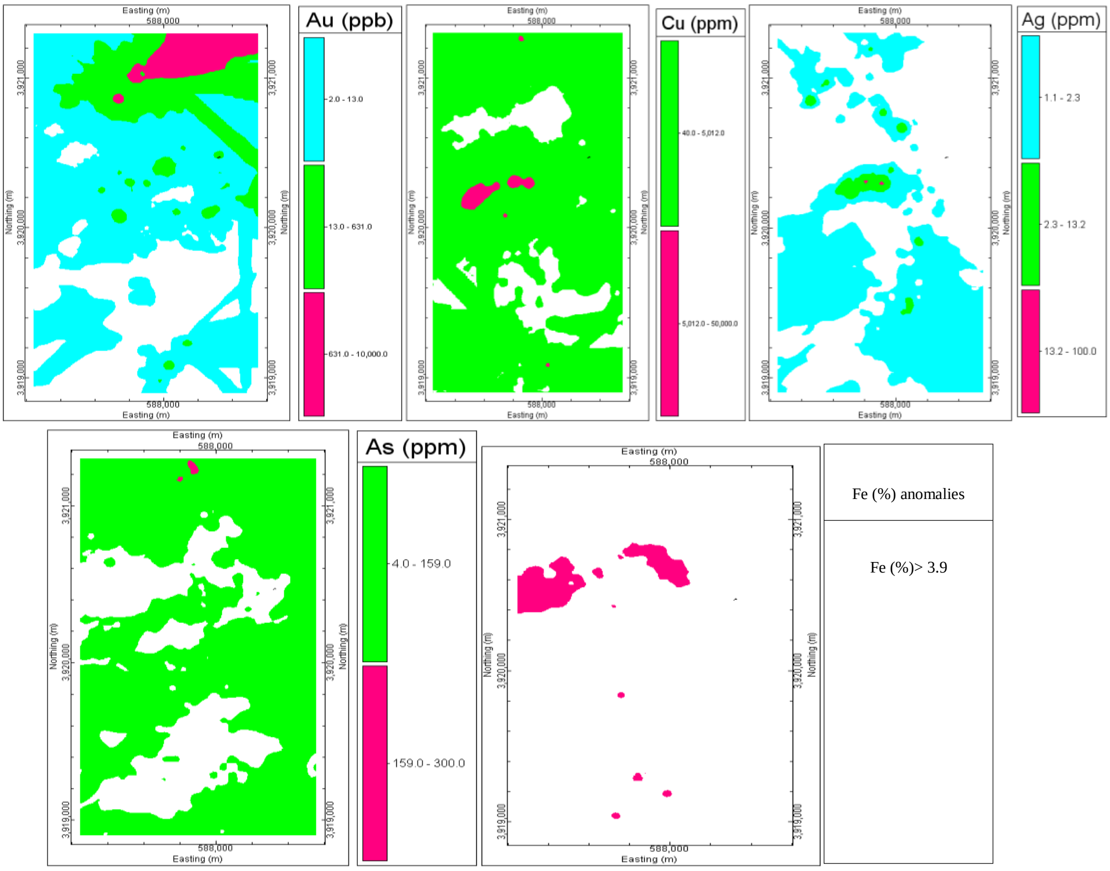

Figure 7. *Au, Cu, Ag, As and Fe geochemical population distribution maps based on C-A method*

5. Comparison with geological particulars

Thresholds and cut-off results from C-A method are compared and correlated to specific geological particulars of the region including considering nature of lithological units, faults and alterations. Au, Cu, Ag, As and Fe distributions in the Bardaskan region, and the faults map are shown in Fig. 8.

The anomalous parts clearly indicate the main identified faults especially in NE and central parts of the area. Comparison between faults positions and elemental anomalies shows that faults intersect the anomalies situated near those structures as depicted in Fig. 8.

On the other hand, faults and elemental anomalies have a proportional relationship. High grade elemental anomalies occurred inside and within the fault zones or located on faults intersection areas (Fig. 8). This is a positive parameter because silicified and quartz-sulfide veins were occurred along these faults and Au particles are existed in these veins.

In this study area, based on results of the C-A method, the elemental anomalies correlated with different rock types.

High amounts of Cu, over 5012 ppm, are highest in sericite and chlorite schists. There are sulfide mineralization especially chalcopyrite. The Au high intensity anomalous, higher than 631 ppb, areas v is situated in tuffaceous sandstones. Also there are quartz veins and veinlets. An epithermal system is existed in this area and correlated within main Au anomalies. Also, the main step Ag mineralization, higher than 2.3 ppm, is correlated within sericite schists as presented in Fig. 8.

Alterations have a strong positive relationship with Cu, Au and Ag anomalies. All of the anomalous parts are covered by chloritization, sericitization and silicification alterations. Most chloritization alteration is associated with Cu anomalies as shown in Fig. 9. Cu with concentration at higher than 40 ppm, Au, higher than 13 ppb, and Ag, higher than 1.1 ppb, do have anomalies in central parts of the area and are covered by chloritization and silicification alterations.

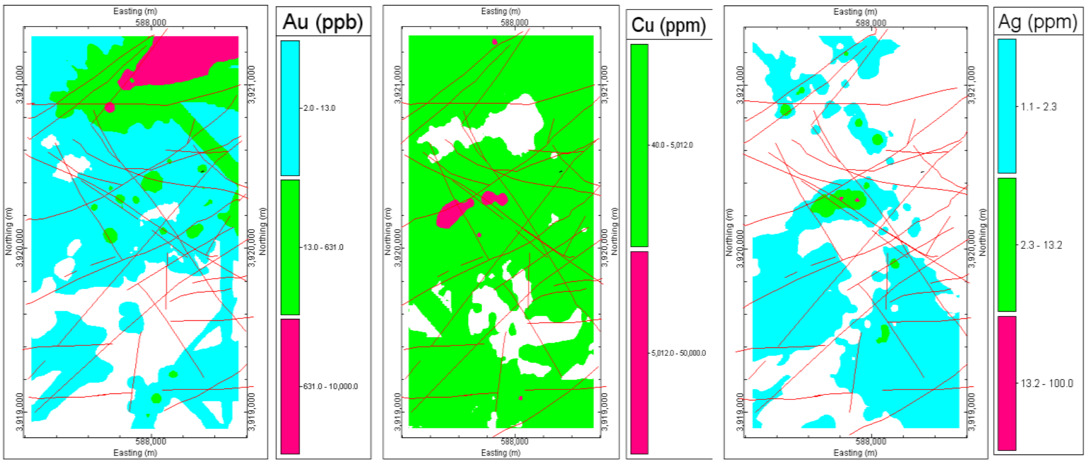

Figure 8. *Elemental geochemical population distribution maps based on C-A method imposed on fault location maps (red lines)*

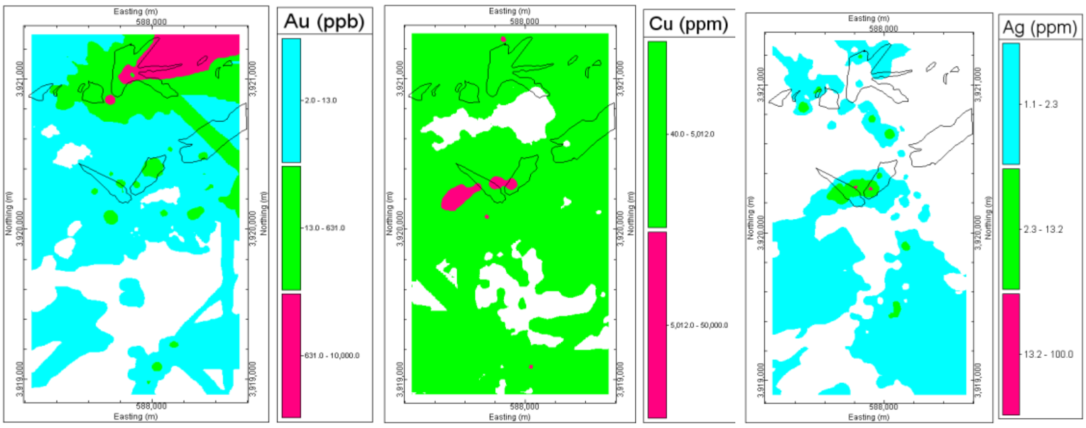

Figure 9. *Relationship between Au, Cu and Ag distribution and sericitization, chloritization and silicification, alterations and sulfide mineralization (polygons)*

Also, chloritization alterations correlate with Cu low intensive anomaly in eastern parts only as shown in Fig. 9. Silicification alterations are correlated within Au high intensity anomalous parts, higher than 631 ppb, in NE parts of the area.

6. Conclusions

The study on Bardaskan area reveals the potential use of the C-A method for geochemical anomaly separation as a useful tool for geochemical and mineral exploration. The advantages of this method relies essentially on its simplicity, and easy computational implementation, as well as the possibility to compute a numerical value of concentrations, i.e., the anomalous threshold, which is the most useful criteria for cross examination of information with numerical data from different sources, commonly used in lithogeochemistry.

There exists a very good correlation between the calculated anomalous threshold values and the geological particulars in the Bardaskan area. These results may also be interpreted differently according to their nature, especially multifractal curves in log-log plots. Cu, Fe and As concentration in the area may be a result of the three steps of enrichment, i.e., mineralization and later dispersions. Au and Ag log-log plots were shown that there is four steps for their mineralization and dispersion. Major Au mineralization occurred in silicificated units in NE parts of the area. Au particles are occurred in quartz and quartz-sulfide veins and veinlets.

The occurrence of Cu and Ag high enrichments in tuffaceous sandstones and chlorite schists in central parts of the area has been actually realized in the samples collected from the field. The studied elements anomalies have proper and direct relationships with faults in Bardaskan area. High intensive elements anomalies are mostly situated at faults intersections. It is important because quartz and quartz-sulfide veins and veinlets are occurred along these faults. There is a good correlation between chloritization and silicification alterations and anomalous concentration, of Au, Cu and Ag. Silicification alteration has good relationships with Au high grade anomalous enrichment parts.

7. References

[1] Agterberg, F.P., Cheng, Q., Brown, A., Good, D., Computers & Geosciences 22 (1996), pp. 497-507.

[2] Alavi, M., Tectonophysics, 229 (1994), pp. 211-238.

[3] Afzal, P., Khakzad, A., Moarefvand, P., Rashidnejad Omran, N., Esfandiari, B., Fadakar Alghalandis, Y., Journal of Geochemical Exploration 104 (2010), pp. 34-46.

[4] Bababkhani, A., Mehrpatu, M., Radfar, J., Majidi, J., Geological and exploration report of Taknar polymetallic deposit, Iranian Geological survey, Tehran, (1999), p. 215.

[5] Bolviken, B., Stokke, P.R., Feder, J., Jossang, T., Journal of Geochemical Exploration 43 (1992), pp. 91-109.

[6] Cheng, Q, Agterberg, F. P., Ballantyne, S. B., Journal of Geochemical Exploration 51 (1994), pp. 109-130.

[7] Cheng, Q., Agterberg, F.P., Mathematical Geology 28 (1996), pp. 1-16.
[8] Cheng, Q., Journal of Geochemical Exploration 65 (1999), pp. 175-194.
[9] Davis, J.C., Statistics and data analysis in Geology (3th ed.), John Wiley & Sons Inc., New York, (2002), p. 638.
[10] Evertz, C.J.G., Mandelbrot, B.B., Multifractal measures (appendix B). In: Peitgen, H.-O., Jurgens, H., Saupe, D. (Eds.). Chaos and Fractals, Springer, New York, (1992), p. 953.
[11] Goncalves, M.A., Vairinho, M., Oliveira, V., Proceeding of IV IAMG'98. De Frede, Ischia Island, Italy, (1998), p. 590.
[12] Goncalves, M.A., Mathematical Geology 33 (2001), pp. 41-61.
[13] Goncalves, M. A., Mateus, A., Oliveira, V., Journal of Geochemical Exploration 72 (2001), pp. 91-114.
[14] Halsey, T.C., Jensen, M.H., Kadanoff, L.P., Procaccia, I., Shraiman, B.I., Physical Review A 33 (1986), pp. 1141-1151.
[15] Li, Ch., Ma, T., Shi, J., Journal of Geochemical Exploration 77 (2003), pp. 167-175.
[16] Lima, A., De Vivo, B., Cicchella, D., Cortini, M., Albanese, S., Applied Geochemistry 18 (2003), pp. 1853-1865.
[17] Mandelbrot, B.B., The Fractal Geometry of Nature, W. H. Freeman, San Fransisco, (1983), p. 468.
[18] Meng, X, Zhao, P., Chinese Journal of Geosciences, 2 (1991), pp. 207-211.
[19] Rafiee, A., 20th World Mining Congress Proceeding, National Geosciences Database of Iran, Tehran, Iran, (2005), p. 461.
[20] Sim, B.L., Agterberg, F.P., Beaudry, C., Computers & Geosciences. 25 (1999), pp. 1023-1041.
[21] Turcotte, D.L., Economic Geology, 18 (1986), pp. 1525-1532.
[22] Wei, Sh., Pengda, Zh., Computers & Geosciences 28 (2002), pp. 369-376.